

VNU Journal of Science: Mathematics - Physics





Original Article

Structural Optimization of 1, 2-dibromoethane-filled Hexagonal Photonic Crystal Fiber Based on As₃₉Se₆₁ Glass for Super-continuum Applications

Le Van Hieu*

Hong Duc University, 565 Quang Trung, Thanh Hoa, Vietnam

Received 16th January 2025 Revised 8th March 2025; Accepted 22nd April 2025

Abstract: In this work, a highly nonlinear chalcogenide photonic crystal fiber (PCF) infiltrated with 1, 2-dibromoethane ($C_2H_4Br_2$) has been numerically proposed to generate a super-continuum application. The proposed PCF exhibits numerous significant optical guiding properties, including dispersion, effective mode area, and nonlinearity. The simulation results show that the optimized PCF with lattice constant $\Lambda=2.0~\mu m$ and filling factor f=0.5 exhibits all normal dispersion regions. The optimized fiber has a maximum point of the dispersion curve at a wavelength of 3.15 μm , which is closest to the pump wavelength of 3.0 μm . At the pump wavelength of 3.0 μm , the optimized fiber has a dispersion value of - 20.05 ps/nm/km, an effective area of 5.88 μm^2 , and a nonlinearity coefficient of 7,837.63 μm^{-1} . This nonlinearity coefficient value is very high compared to other fibers. The estimated parameters are suitable for further simulation and investigation of the design for broadband super-continuum generation.

Keywords: Photonic crystal fiber, dispersion characteristics, chalcogenide, liquids.

1. Introduction

Photonic crystal fibers (PCFs), also known as holey or microstructure fibers, have attracted increasing attention in recent years due to their outstanding optical properties and flexibility in structural design [1]. PCFs can exhibit many high-performance properties, such as endless single-mode operation [2], high birefringence [3], high nonlinearity, and controllable chromatic dispersion [4, 5], by varying the cladding arrangement. Among these features of PCF, highly nonlinear PCFs are suitable for various novel applications, including optical communication, fiber lasers and amplifiers, and super-continuum (SC) generation [6, 7].

E-mail address: levanhieu@hdu.edu.vn

^{*} Corresponding author.

In such PCFs, the control of chromatic dispersion is an important property because it is an important issue in optical fiber communication systems. The dispersion properties and dispersion slope always have a strong effect on the nonlinear coefficient [8]. So far, many types of PCFs have been proposed to study dispersion and nonlinearity. Among the cladding air hole arrangements, the hexagonal lattice arrangement or deformations based on it, in which the air holes have a fixed hole-to-hole spacing, are the most widely used [8, 9]. In addition to the hexagonal arrangement of air holes, other structures, such as square lattices and octagonal structures or structures with different diameters of air holes, have also been proposed as PCF designs [4, 10, 11]. Although some good results with flat dispersion and high nonlinearity have been obtained, these structures pose challenges in fabrication.

Recently, the infiltration of PCFs with liquids has provided additional freedom for expanding applications in potential fields [12, 13], particularly with the use of SC laser sources in medical diagnostics and biomedical technologies [14, 15]. The advantage of using PCFs with a liquid core or filled cladding is that the dispersion properties of the PCFs can be altered by changing temperature or pressure [16]. Another advantage is that some liquids, e.g., carbon disulfide (CS₂), C₂H₄Br₂ are very transparent in the near-IR region [17, 18]. Furthermore, nonlinear liquids are highly nonlinear compared to nonlinear soft glasses [19, 20].

In this work, the chromatic dispersion, effective area, and nonlinearity of the PCF are numerically analyzed based on the full-vector finite element method (FEM). The designed PCF is made of pure $As_{39}Se_{61}$ glass with all air holes in the cladding infiltrated with $C_2H_4Br_2$. The PCF has a modest number of parameters, including six rings with the same air hole diameters and only one air hole pitch, but it can provide relatively optimal properties. The optimized design has all-normal dispersion ranges by optimizing the parameters of the fiber structure. The optimized fiber has a maximum point of the dispersion curve at a wavelength of 3.15 μ m with a peak value of -18.02 ps/nm/km, which is closest to the pump wavelength of 3.0 μ m. At the pump wavelength of 3.0 μ m, the optimized fiber has a dispersion value of -20.05 ps/nm/km, an effective area of 5.88 μ m², and a nonlinearity coefficient of 7837.63 w⁻¹km⁻¹.

2. The Photonic Crystal Fiber Design

To begin, we design a PCF structure with which we can generate broadband SC spectra in the midinfrared (IR). Since the aim is to create broadband SC with a very short PCF at low input power, we developed the design so that the PCF has a large effective nonlinearity with all normal dispersion regions. Moreover, the wavelength corresponding to the maximum point of the dispersion of the fiber should be very close to the pump wavelength of 3.0 μ m. In this design, we used a full-vector FEM combined with perfectly matched layer boundary conditions to analyze the properties of the fiber. The wavelength-dependent refractive index of optical material is calculated using a Sellmeier equation and is directly included in the simulation [13]:

$$n = \sqrt{A_0 + \frac{B_1 \lambda^2}{\lambda^2 - C_1} + \frac{B_2 \lambda^2}{\lambda^2 - C_2}} \tag{1}$$

where the constants B_i and C_i (i = 1, 2) in the Sellmeier equation for these materials are listed in Table 1.

 $C_2 \left[\mu m^2 \right]$ Coefficient A_0 B_1 B_2 C_{I} [μm^{2}] As₃₉Se₆₁ [21] 3.7464 3.9057 3.9057 0.16589 1606.56 1.31637 0.401322 0.0161612 142.2298902 C₂H₄Br₂ [18]

Table 1. Sellmeier coefficients of materials used

Figure 1a shows the proposed PCF structure's cross-section. The material is As₃₉Se₆₁ glass, and the number of air-hole rings is assumed to be 6. It consists of circular air holes arranged in a regular hexagon

array with the lattice constant Λ , with the central air hole missing, and all air holes have a uniform diameter d and are filled with C₂H₄Br₂. We selected As₃₉Se₆₁ glass because this glass provides a high nonlinear refractive index ($n_2 = 2.2 \times 10^{-17} \text{ m}^2/\text{W}$ [21]), and high transparency [21]. Meanwhile, $C_2H_4Br_2$ is very transparent in the near-IR region [18]. Figure 1b shows the mode field intensity distribution of the fiber at 1.0 µm wavelength corresponding to the optimal design. It is apparent that the mode is well confined in the core region and can remain endlessly in a single mode over a wide wavelength range.

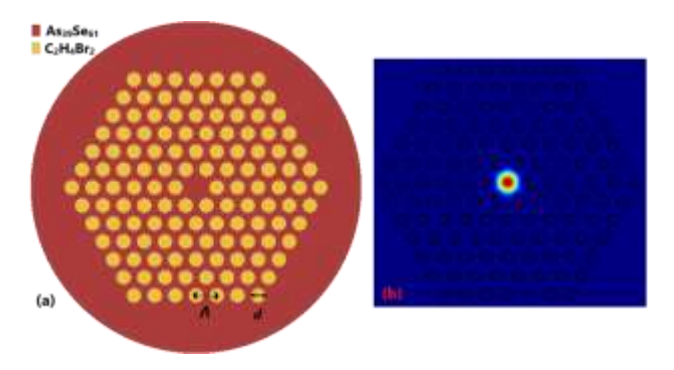


Figure 1. (a) Schematic of the modeled PCF structure, (b) the fundamental electric field properties for x-polarization mode at 1.0 μ m, with parameters of $\Lambda = 2.0 \mu$ m, and $d = 1.0 \mu$ m.

3. Dispersion Engineering and Analysis

The chromatic dispersion is one of the most important parameters relevant to optical applications, as it may strongly affect the performance of communication systems. The total dispersion of the fiber is the sum of waveguide dispersion D_w and material dispersion D_m [22]:

$$D(\lambda) = D_w(\lambda) + D_m(\lambda) \tag{2}$$

$$D_{w}(\lambda) = -\frac{\lambda}{c} \frac{d^{2}Re[n_{eff}]}{d\lambda^{2}}$$

$$D_{m}(\lambda) = -\frac{\lambda}{c} \frac{d^{2}n_{m}}{d\lambda^{2}}$$

$$(3)$$

$$D_m(\lambda) = -\frac{\lambda}{c} \frac{d^2 n_m}{d\lambda^2} \tag{4}$$

where λ is the operating wavelength, where $Re[n_{eff}]$ is the real part of the refractive index, c is the speed of light, n_{eff} is the effective refractive index of the fiber. Material dispersion $D_m(\lambda)$ can be calculated with the Sellmeier equation.

The variation of the dispersion with the wavelength of the designed fiber is shown in Fig. 2 for different values of the lattice constant Λ from 1.5 μ m to 2.5 μ m, step of 0.5 μ m, and filling factor f from 0.3 to 0.8 with step of 0.1. It can be seen from this figure that the dispersion of the fiber increases significantly for a given Λ when the filling factor is increased (the size of the hole diameter in the cladding decreases), as seen in Figs. 2(a)-(c). Increasing the fill factor f can shift the dispersion properties from normal to anomalous regions. By increasing the f of 0.3, 0.4, 0.5, 0.6, 0.7 and 0.8, the value of chromatic dispersion in the anomalous region of the mid-IR region can be obtained -197.44 ps/nm/km, -124.47 ps/nm/km, -55.069 ps/nm/km, -3.62 ps/nm/km, 40.98 ps/nm/km and 86.8699 ps/nm/km at a wavelength of 2.83 μ m when Λ is equal to 1.5 μ m. In particular, the zero-dispersion wavelength (ZDW) of the fiber moves to smaller wavelengths as the filling factor increases. For a given value of filling factor f, a significant reduction in the dispersion is possible for fibers with increases Λ , and the ZDW of this fiber can be shifted towards longer wavelengths by increasing the lattice constant Λ , as seen in Fig. 2(d). With $\Lambda = 1.5 \,\mu\text{m}$, f = 0.8, the fiber has a zero point of dispersion of 2.42 μm , while these values are 2.53 μm and 2.85 μ m for fiber with $\Lambda = 2.0 \mu$ m, f = 0.8 and fiber with $\Lambda = 2.5 \mu$ m, f = 0.8, respectively.

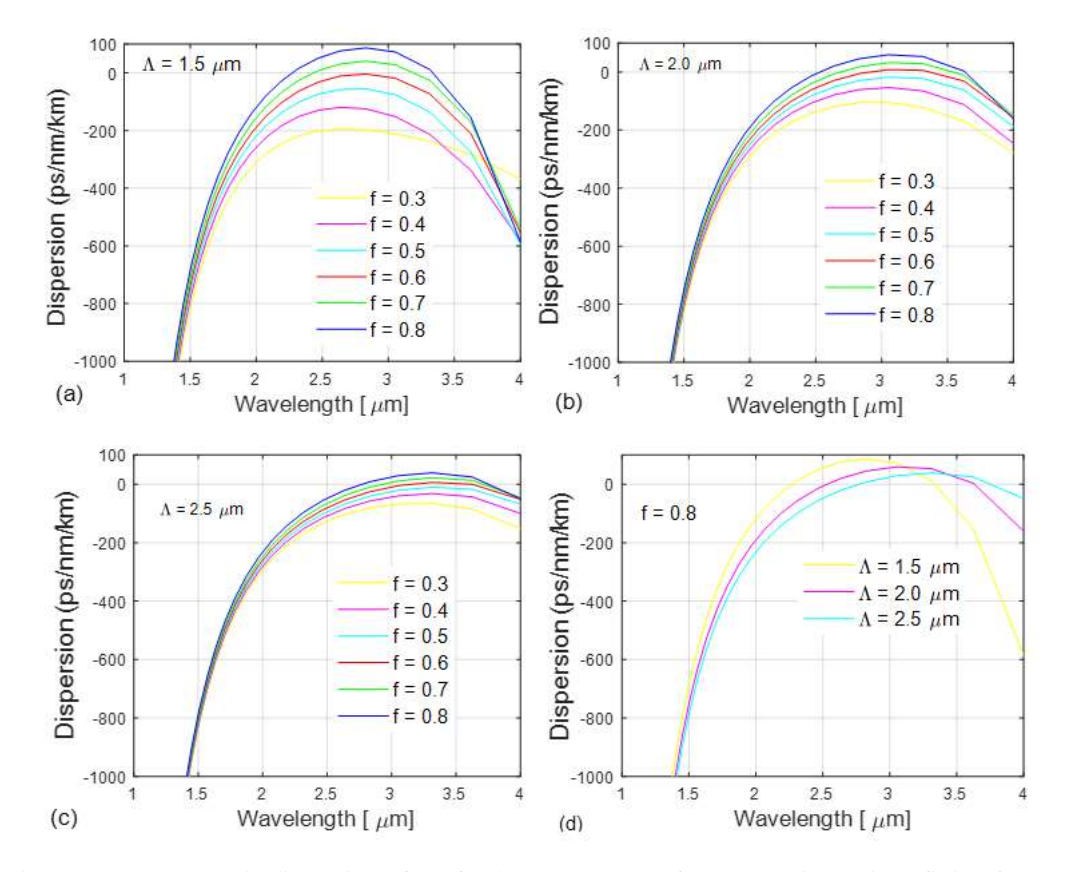


Figure 2. The chromatic dispersion of the fundamental mode of the PCF with various filling factors f, and lattice constant Λ .

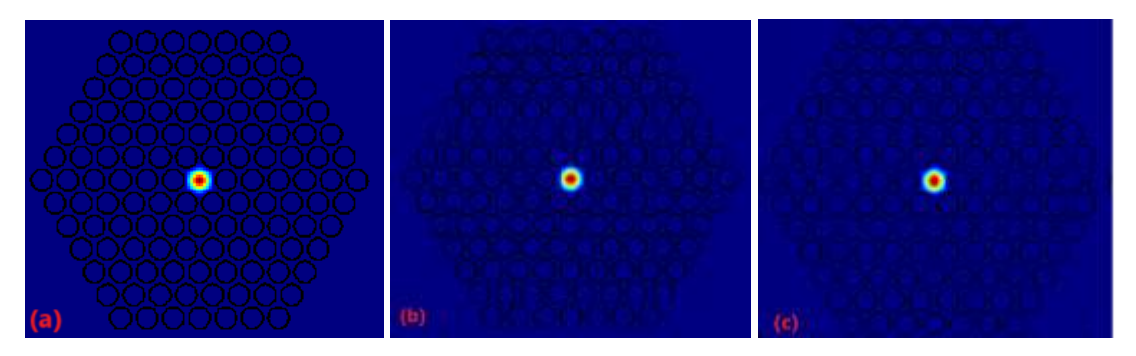
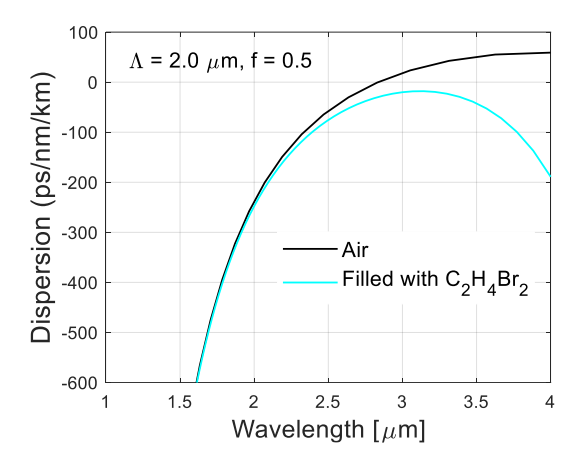


Figure 3. The fundamental electric field properties for x-polarization mode at 1.0 μ m, with parameters of $\Lambda = 1.5 \mu$ m, and $d = 1.2 \mu$ m, $\Lambda = 2.0 \mu$ m, and $d = 1.6 \mu$ m and $\Lambda = 2.5 \mu$ m, and $d = 2.0 \mu$ m.

Fig. 3 shows an example of the electric field distribution of fiber with various lattice constants and filling factor f = 0.8. As a result, the mode field has been maintained in the core. As the lattice constant increases, more light is focused into the core, and less is lost to the outside.

Based on the above analysis, the optimal geometric parameters are determined: $\Lambda = 2.0 \ \mu m$, f = 0.5, and $d = 1.0 \ \mu m$. The optimized PCF produces all normal dispersion regions where the point of maximum dispersion is closest to the x-axis, and its peak equals -18.02 ps/nm/km at 3.15 μm , closest to the pump wavelength of 3.0 μm . Moreover, the optimal size fiber, i.e., when the holes are not filling with liquid, is characterized by anomalous dispersion where ZDW is equal to 2.85 μm , as shown in Fig. 4.



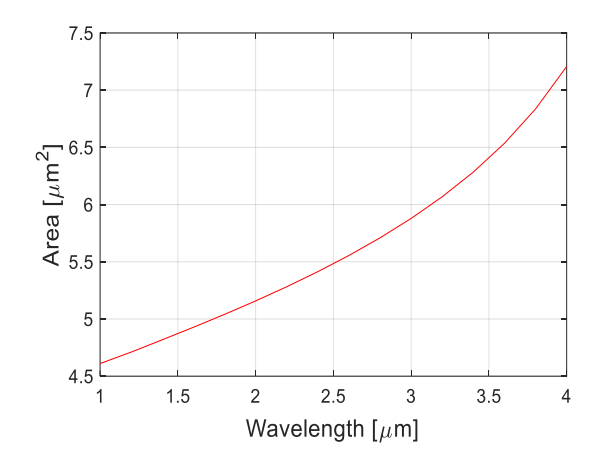


Figure 4. Numerical simulations of the characteristic dispersion in the optimized PCF with air holes, and filled with $C_2H_4Br_2$.

Figure 5. The effective mode area curve for wavelengths of the proposed PCF.

The effective mode area of the optimized PCF is an important parameter for the calculation of the nonlinearity. The effective mode area, A_{eff} for the optimized PCF can also be calculated using the following formula: $A_{eff} = \frac{(\iint |E|^2 dx dy)^2}{\iint |E|^4 dx dy}$, where E(x,y) in the formula is the transverse electric field component. Figure 5 shows a variation of the effective mode area with wavelength. It is clear that the effective mode area increases with increasing wavelength. The effective mode area is 5.88 μ m² at a wavelength of 3.0 μ m.

The highly nonlinear PCF is more suitable for practical applications because the value of optical nonlinearity depends mainly on the size of the core and the different configurations of the air holes in the PCF. The nonlinearity depends on the effective area of the fiber structure and is inversely proportional to the effective area according to the formula: $\gamma(\lambda) = \frac{2\pi n_2}{\lambda A_{eff}}$, where n_2 is a nonlinear refractive index of the fiber.

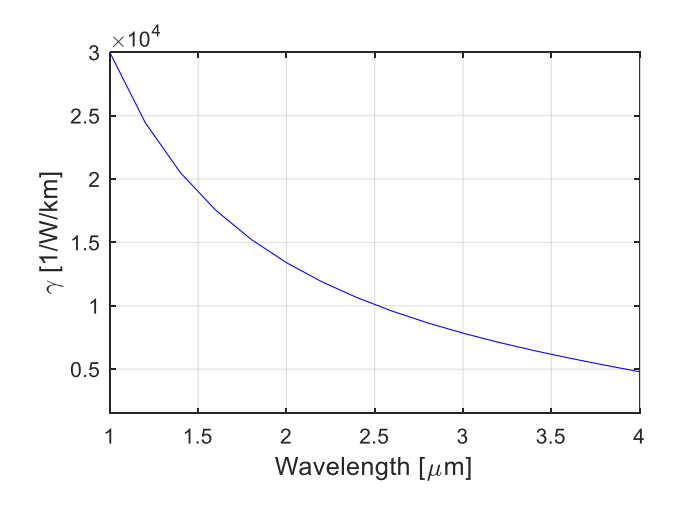


Figure 6. The nonlinear coefficient curve for wavelengths of the proposed PCF.

Fig. 6 shows the wavelength-dependent nonlinear coefficient in the optimized fiber. The graph shows a unique pattern that illustrates the fluctuation of the nonlinear coefficient at different wavelengths. The result is that the nonlinear coefficient in the optimized fiber decreases with increasing wavelength. The nonlinearity is 7,837.63 w⁻¹km⁻¹ at a wavelength of 3.0 μm. The optimized fiber has a very high nonlinear coefficient compared to other fibers [13, 23, 24]. Although the proposed fiber cannot achieve ultra-flat dispersion properties compared to the work [25], or obtain the same flat-dispersion properties compared to the work [26], this fiber structure also has a higher nonlinear coefficient.

4. Conclusion

In this study, a new PCF design was proposed to extend the super-continuum generation in the midinfrared region. The proposed design was made of $As_{39}Se_{61}$ glass as the background material, which has a very high nonlinear refractive index ($n_2 = 2.2 \times 10^{-17}$ m²/W), and all air holes were infiltrated with $C_2H_4Br_2$. The proposed PCF design consisted of six rings of circular air holes arranged in a hexagonal lattice. The geometrical parameters of the PCF design were modified to achieve an all-normal dispersion regime. According to the simulations performed, the optimized PCF with a lattice constant $\Lambda = 2.0 \mu m$ and filling factor f = 0.5, the optimized fiber exhibits an all-normal dispersion, with a peak value of -18.02 ps/nm/km at $3.15 \mu m$. The dispersion, the effective mode area (A_{eff}), and the nonlinear coefficient (γ) at the wavelength $\lambda = 3.0 \mu m$ are estimated to be -20.05 ps/km/nm, $5.88 \mu m^2$, and $7.837.63 \text{ w}^{-1} \text{km}^{-1}$, respectively, for the optimized PCF. The investigation results are suitable for further investigation of the design for broadband super-continuum generation.

References

- [1] Y. Huang, H. Yang, S. Zhao, Y. Mao, S. Chen, Design of Photonic Crystal Fibers with Flat Dispersion and Three Zero Dispersion Wavelengths for Coherent Supercontinuum Generation in Both Normal and Anomalous Regions, Results in Physics., Vol. 23, 2021, pp. 104033, https://doi.org/10.1016/j.rinp.2021.104033.
- [2] J. C. Knight, T. A. Birks, P. S. J. Russell, D. M. Atkin, All-Silica Single-Mode Optical Fiber with Photonic Crystal Cladding, Opt. Lett., Vol. 21, 1996, pp. 1547-1549, https://doi.org/10.1364/OL.21.001547.
- [3] S. M. A. Razzak, Y. Namihira, Highly Birefringent Photonic Crystal Fibers with Near-Zero Dispersion at 1550 nm Wavelength, J. Mod. Opt., Vol. 56, 2009, pp. 1188-1193, https://doi.org/10.1080/09500340902994132.
- [4] S. M. A. Razzak, Y. Namihira, Proposal for Highly Nonlinear Dispersion-Flattened Octagonal Photonic Crystal Fibers, IEEE Photon. Technol. Lett., Vol. 20, 2008, pp. 249-251, https://doi.org/10.1109/LPT.2007.912986.
- [5] T. Matsui, J. Zhou, K. Nakajima, I. Sankawa, Dispersion Flattened Photonic Crystal Fiber With Large Effective Area and Low Confinement Loss, J. Light wave Technol., Vol. 23, No. 12, 2005, pp. 4178–4183, https://opg.optica.org/jlt/abstract.cfm?URI=jlt-23-12-4178.
- [6] B. Kaur, S. Kumar, B. K. Kaushik, Advances in Photonic Crystal Fiber: Sensing and Supercontinuum Generation Applications, Opt. Fiber Technol., Vol. 72, 2022, pp. 102982, https://doi.org/10.1016/j.yofte.2022.102982
- [7] K. Saitoh, M. Koshiba, Highly Nonlinear Dispersion Flattened Photonic Crystal Fibers For Supercontinuum Generation In A Telecommunication Window, Opt. Express., Vol. 12, No. 10, 2004, pp. 2027-2032, https://doi.org/10.1364/OPEX.12.002027.
- [8] T. L. Wu, C. H. Chao, A Novel Ultra-Flattened Dispersion Photonic Crystal Fiber, IEEE Photon. Technol. Lett., Vol. 17, No.1, 2005, pp. 67-69, https://doi.org/10.1109/LPT.2004.837475.
- [9] M. J. M. Zamani, M. Rouzbahani, Highly Efficient Hybrid-Structured Photonic Crystal Fiber with Ultra-Low Loss and Near-Zero Flat Dispersion for Terahertz Waveguiding, Opt. Quantum Electron., Vol. 56, 2024, pp. 1362, https://doi.org/10.1007/s11082-024-07258-x.
- [10] N. V. T. Minh, L. C. Van, P. N. Thi Hong, V. T. Hoang, H. T. Nguyen, H. V. Le, Supercontinuum Generation in A Square-Lattice Photonic Crystal Fiber Using Carbon Disulfide Infiltration, Optik., Vol. 286, 2023, pp. 171049, https://doi.org/10.1016/j.ijleo.2023.171049.

- [11] K. Kaneshima, Y. Namihira, N. Zou, H. Higa, Y. Nagata, Numerical Investigation of Octagonal Photonic Crystal Fibers With Strong Confinement Field, IEICE Trans. Electron., Vol. E89-C, No. 6, 2006, pp. 830–837, doi: 10.1093/ietele/e89-c.6.830.
- [12] R. Raei, M. Ebnali-Heidari, H. Saghaei, Supercontinuum Generation In Organic Liquid-Liquid Core Cladding Photonic Crystal Fiber in Visible and Near-Infrared Regions, J. Opt. Soc. Am. B., Vol. 35, No. 2, 2018, pp. 0740-3224, https://doi.org/10.1364/JOSAB.35.000323.
- [13] H. V. Le, V. T. Hoang, G. St epniewski, T. L. Canh, N. V. T. Minh, R. Kasztelanic, M. Klimczak, J. Pniewski, K. X. Dinh, A. M. Heidt, R. Buczy'nski, Low Pump Power Coherent Supercontinuum Generation in Heavy Metal Oxide Solid-Core Photonic Crystal Fiber Infiltrated with Carbon Tetrachloride Covering 930 2500 nm, Opt. Express., Vol. 29, No. 24, 2021, pp. 39587-39601, https://doi.org/10.1364/JOSAB.35.000323.
- [14] F. Begum, Y. Namihira, Design of Supercontinuum Generating Photonic Crystal Fiber at 1.06, 1.31 and 1.55 μm Wavelengths for Medical Imaging and Optical Transmission Systems, Natural Science., Vol. 3, No. 5, 2011, pp. 401-407, https://doi.org/10.4236/ns.2011.35054.
- [15] A. Labruyere, A. Tonello, V. Couderc, G. Huss, P. Leproux, Compact Supercontinuum Sources and Their Biomedical Applications, Opt. Fiber Technol., Vol. 18, No. 2, 2012, pp. 375-378, https://doi.org/10.1016/j.yofte.2012.08.003.
- [16] H. L. Van, R. Buczynski, V. C. Long, M. Trippenbach, K. Borzycki, A. N. Manh, R. Kasztelanic, Measurement of Temperature and Concentration Influence on the Dispersion of Fused Silica Glass Photonic Crystal Fiber Infiltrated with Water–Ethanol Mixture, Opt. Commun., Vol. 407, 2018, pp. 417–422, https://doi.org/10.1016/j.optcom.2017.09.059.
- [17] D. Churin, T. N. Nguyen, K. Kieu, R. A. Norwood, N. Peyghambarian, Mid-IR Supercontinuum Generation in An Integrated Liquid-Core Optical Fiber Filled With CS2, Opt. Mater. Express., Vol. 3, No. 9, 2013, pp. 1358-1364, https://doi.org/10.1364/OME.3.001358.
- [18] H. L. Van, V. T. Hoang, T. L. Canh, Q. H. Dinh, H. T. Nguyen, N. V. T. Minh, M. Klimczak, R. Buczynski, R. Kasztelanic, Silica-Based Photonic Crystal Fiber Infiltrated with 1,2-dibromoethane for Supercontinuum Generation, Appl. Opt., Vol. 60, No. 24, 2021, pp. 7268-7278, https://doi.org/10.1364/AO.430843.
- [19] T. K. Phan, L. D. Vu, H. P. T. Nguyen, Y. Ohishi, Coherent Mid-Infrared Supercontinuum Seneration in Tellurite All-Solid Microstructured Optical Fibers with Anomalous and Normal Dispersion Property, Results Opt., Vol. 13, 2023, pp. 100576, https://doi.org/10.1016/j.rio.2023.100576.
- [20] H. Pakarzadeh, Z. Fatemipanah, U. A. Kumar, Supercontinuum Generation In Silica-Based Photonic Crystal Fibers For High-Resolution Ophthalmic Optical Coherence Tomography, Silicon., Vol. 15, 2023, pp. 6655-6661, https://doi.org/10.1007/s12633-023-02533-0.
- [21] X. Yang, J. Yang, Q. Xu, H. Yang, Super-Flat Coherent Mid-Infrared Supercontinuum in All-Normal Dispersion As39Se61 Chalcogenide Photonic Crystal Fiber, Phys. Scr., Vol. 98, 2023, pp. 125512, https://doi.org/10.1088/1402-4896/ad0a2f.
- [22] Y. Wang, X. Zhang, X. Ren, L. Zheng, X. Liu, Y. Huang, Design and Analysis of A Dispersion Flattened and Highly Nonlinear Photonic Crystal Fiber with Ultralow Confinement Loss, Applied optics., Vol. 49, No. 3, 2010, pp. 292-297, https://doi.org/10.1364/AO.49.000292.
- [23] H. V. Le, Coherence Evolution of Multi-Pulse Pumped Super-continuum in Multicomponent GeSe2-As2Se3-PbSe Chalcogenide Photonic Crystal Fiber with Four Zero-Dispersion Wavelengths, Journal of the Optical Society of America B., Vol. 41, No. 12, 2024, pp. 2780-2790, https://doi.org/10.1364/JOSAB.539742.
- [24] T. K. Phan, L. D. Vu, H. P. T. Nguyen, Y. Ohishi, Coherent Mid-Infrared Supercontinuum Generation in Tellurite All-Solid Microstructured Optical Fibers with Anomalous and Normal Dispersion Property, Results Opt., Vol. 13, 2023, pp. 100576, https://doi.org/10.1016/j.rio.2023.100576.
- [25] T. T. B. Le, T. D. Van, L. C. Van, T. N. T. Ha, D. H. Trong, T. N. Thi, Nonlinear Properties of Circular Solid-Core Photonic Crystal Fiber With The Difference of Air-Hole Diameters and the Spacing of Air-Holes in the Cladding, Hue University Journal of Science: Natural Science., Vol. 131, No. 1D, 2022, pp. 13–21, https://doi.org/10.26459/hueunijns.v131i1D.6685.
- [26] V. T. M. Ngoc, T. V. Thanh, C. T. H. Sam, L. T. B. Tran, D. V. Trong, N. T. Thuy, L. V. Hieu, C. V. Lanh, Optimization Of Optical Properties Of Ge20Sb5Se75-Based Photonic Crystal Fibers, Vinh University Journal of Science., Vol. 51, No. 3A, 2022, pp. 12-21, DOI: 10.56824/vujs.2022nt16.